Development of Structural Health Monitoring Systems Incorporating Acoustic Emission Detection for Spacecraft and Wind Turbine Blades

Jinsik Yun

Thesis submitted to the faculty of the
Virginia Polytechnic Institute and State University
In partial fulfillment of the requirements for the degree of

Master of Science
In
Electrical Engineering

Dong S. Ha, Chair
Daniel J. Inman
Patrick Schaumont

April 28, 2011
Blacksburg, VA

Key words: Structural Health Monitoring, Acoustic Emission, Impedance-Based SHM, Wireless Sensor Network

Development of Structural Health Monitoring Systems Incorporating Acoustic Emission Detection for Spacecraft and Wind Turbine Blades

Jinsik Yun

(Abstract)

Structural Health Monitoring (SHM) is the science and technology of monitoring and can assess the condition of aerospace, civil, and mechanical infrastructures using a sensing system integrated into the structure. SHM is capable of detecting, locating, and quantifying various types of damage such as cracks, holes, corrosion, delamination, and loose joints, and can be applied to various kinds of infrastructures such as buildings, railroads, windmills, bridges, and aircraft.

A major technical challenge for existing SHM systems is high power consumption, which severely limits the range of its applications. In this thesis, we investigated adoption of acoustic emission detection to reduce power dissipation of SHM systems employing the impedance and the Lamb wave methods. An acoustic emission sensor of the proposed system continuously monitors acoustic events, while the SHM system is in sleep mode. The SHM system is evoked to perform the SHM operation only when there is an acoustic event detected by the acoustic emission sensor. The proposed system avoids unnecessary operation of SHM operations, which saves power, and the system is effective for certain applications such as spacecraft and wind turbine blades. We developed prototype systems using a Texas Instruments TMS320F2812 DSP evaluation board for the Lamb wave method and an MSP430 evaluation board for the impedance method.

Acknowledgement

I would like to express my deepest gratitude to my advisor, Dr. Dong S. Ha, for his constant guidance and support in advising me to conduct and complete this work. I am also grateful to him for taking care of me ever since I first came into the US. Without his sincere helps, my graduate life would not have been successful, and this thesis not have completed.

I would also like to thank Dr. Daniel J. Inman for giving me his generous support so that I could start my academic research on the SHM, and now I can finish the research. I would like to thank Dr. Patrick Schaumont for always allowing me to have his kind guidance on my academic career, and sharing his experiences with me. I would like to thank Dr. Robert Owen of the Extreme Diagnostics for organizing the AED projects and helping me stay on the right track during the execution of the projects.

I would like to thank all VTVT members as well. It was a great pleasure to work and study with them. I would especially like to give my appreciation to Jeongki Kim, Dao Zhou, and Kevin Zeng since their helps on my research were so much valuable.

Finally, I would like to thank my wife, Jihoon, for her endless love and support throughout the whole graduate life. Just being with her is the most essential source of my energy and my life. I also want to give the thank you message to my baby who will be born soon. My baby allows me to have another energy source making me smile all the time.

Table of Contents

List of Figures

List of Tables

Chapter 1: Introduction

The SHM is the science and technology of monitoring and assessing the condition of aerospace, civil, and mechanical infrastructures using a sensing system integrated into the structure. SHM is capable of detecting, locating, and quantifying various types of damage such as cracks, holes, corrosion, delamination, and loose joints, and can be applied to various kinds of infrastructures such as buildings, railroads, windmills, bridges, and aircraft.

A variety of approaches to SHM have been proposed and investigated. The impedance-based method based on using piezoelectric wafers, such as PZT (Lead Zirconate Titanate), is proven to be effective for in situ local damage detection. Since impedance-based systems that are used for SHM typically consist of a digital-to-analog converter (DAC), an analog-to-digital converter (ADC), and processing unit, general impedance-based systems are complicate and power hungry. To address the problem, we investigated a new impedance-based SHM method, which performs SHM operations in the digital domain.

One limitation of the impedance method is its inability to locate the defect, and the Lamb wave propagation method addresses the limitation. The Lamb wave method launches an elastic wave through the structure. The changes in both the wave attenuation and the reflection are sensed to detect and locate damage on surfaces. We investigated a power efficient Lamb wave method, which eliminates a power hungry ADC.

Based on the proposed impedance-based and Lamb wave SHM systems, the AED has been devised, in which an acoustic sensor is added to our SHM systems. An acoustic sensor continuously monitors acoustic events, while the impedance-based and Lamb wave SHM systems are in sleep mode. The SHM systems are activated only when there is an acoustic event. From these functionalities, we could obviate unnecessary power losses by skipping unwanted repetitions of power hungry SHM operations. As an acoustic sensor dissipates much smaller power compared with the impedance-based and the Lamb wave SHM systems, the use of an acoustic sensor reduces overall power dissipation of the system.

Based on the above considerations, this thesis is outlined as follows. In Chapter 2, our proposed impedance-based and Lamb wave SHM systems are explicated in detail at the preliminary part, and the AED system is applied for spacecraft whose damage is often due to collision of meteorites or space debris. In Chapter 3, this AED system is applied to the WTB to monitor and control the fatigue lifespan of the WTB. Since the AED system is integrated with the wireless sensor network, the operational mechanism for the wireless sensor network is dealt with in detail as well as the AED system. Chapter 4 concludes the work in this thesis.

Chapter 2: Adverse Event Detection (AED) System for Continuously Monitoring and Evaluating Structural Health Monitoring

Structural damage for spacecraft is mainly due to impacts such as collision of meteorites or space debris. We present the SHM system for space applications, named Adverse Event Detection (AED), which integrates an acoustic sensor, an impedance-based SHM system, and a Lamb wave SHM system. With these three health-monitoring methods in place, we can determine the presence, location, and severity of damage. An acoustic sensor continuously monitors acoustic events, while the impedance-based and Lamb wave SHM systems are in sleep mode. If an acoustic sensor detects an impact, it activates the impedance-based SHM. The impedance-based system determines if the impact incurred damage. When damage is detected, it activates the Lamb wave SHM system to determine the severity and location of the damage. Further, since an acoustic sensor dissipates much less power than the two SHM systems and the two systems are activated only when there is an acoustic event, our system reduces overall power dissipation significantly. Our prototype system demonstrates the feasibility of the proposed concept.

2.1 Introduction

Structural Health Monitoring (SHM) is the science and technology of monitoring and assessing the condition of aerospace, civil, and mechanical infrastructures using a sensing system integrated into the structure. SHM is capable of detecting, locating, and quantifying various types of damage such as cracks, holes, corrosion, delamination, and loose joints, and can be applied to various kinds of infrastructures such as buildings, railroads, windmills, bridges, and aircraft. To detect or locate various types of defects, it necessitates an SHM system to employ different SHM methods [2]. However, most existing SHM systems employ only one type of SHM methods targeting specific damages

[3],[4]. To cover different types of damages, we need multiple such SHM systems, resulting in an increased form factor, power consumption, and cost.

A variety of approaches to SHM have been proposed and investigated. The impedance-based method based on using piezoelectric wafers, such as PZT (Lead Zirconate Titanate), is proven to be effective for in situ local damage detection [4]. An impedance-based SHM system performs three major operations: excitation signal generation, sensing the response signal, and damage assessment. The excitation signal for existing SHM systems is typically a sweeping sinusoidal signal, which is generated with a DAC. The response signal is captured by an ADC and processed by a Digital Signal Processing (DSP) chip or a Micro Controller Unit (MCU). Existing impedance-based systems are complicate and power hungry. To address the problems, we investigated a new impedance-based SHM method, which performs SHM operations in the digital domain [4]-[6]. Our system excites a PZT patch with a train of rectangular pulses instead of a sinusoidal signal, which eliminates a DAC. Our system senses only the phase, not the magnitude, of the response signal to eliminate an ADC. Therefore, our system is much simpler in hardware and dissipates far less power.

One limitation of the impedance method is its inability to locate the defect, and the Lamb wave propagation method addresses the limitation. The Lamb wave method launches an elastic wave through the structure. The changes in both wave attenuation and reflection are sensed to detect and locate damage on surfaces [7],[8]. We investigated a power efficient Lamb wave method, which eliminates a power hungry ADC [9]. We also investigated integration of both the impedance-based and Lamb wave methods into a single SHM system [2]. A Hanning windowed sinusoidal signal is generated to excite a Lamb wave for our integrated system. A Hanning windowed sinusoidal signal has a small frequency bandwidth [10], so the generated Lamb waves are limited to the fundamental mode. We applied a discrete wavelet transform to the sensed response, which reduces processing complexity and the memory requirement compared with other transformations such as Fast Fourier Transform (FFT). Since both the impedance and the Lamb wave methods can share a processor and piezoelectric patches, our integrated SHM system reduces the form factor and the power dissipation.

High power consumption of SHM systems is problematic for many SHM

applications including spacecraft. In this paper, we present a low power SHM system, named Adverse Event Detection (AED), in which an acoustic sensor is added to our integrated SHM system employing both the impedance-based and the Lamb wave methods. Our AED system intends for spacecraft whose damage is often due to collision of meteorites or space debris. With these three health-monitoring methods, we can determine the presence, location, and severity of damage. The acoustic sensor continuously monitors acoustic events such as collision of meteorites. If an acoustic sensor detects an impact, it activates the impedance-based SHM system. The impedance-based system determines if the impact incurred damage. When damage is detected, the impedance-based system activates the Lamb wave SHM system to determine the severity and location of the damage. An acoustic sensor continuously monitors acoustic events, while the impedance-based and Lamb wave SHM systems are in sleep mode. The two SHM systems are activated only when there is an acoustic event. As an acoustic sensor dissipates much smaller power compared with the impedance-based and the Lamb wave SHM systems, use of an acoustic sensor reduces overall power dissipation of the system.

The paper is organized as follows. Section 2 reviews briefly the impedance-based and the Lamb wave-based SHM systems. Section 3 describes the operation, architecture, and prototype of our AED system. Section 4 presents experimental results, and Section 5 summarizes our work.

2.2 Preliminaries

We review the impedance-based and the Lamb wave SHM systems employed in our AED system in this section. We also describe the acoustic sensor used for our system.

2.2.1 Impedance-Based SHM System

Analog Device, Inc. introduced an impedance analyzer chip AD5933, which dissipates about 30 mW. The chip includes a DAC to generate an excitation signal up to 100 kHz, a 12-bit ADC, and supports on-chip FFT operation. Park et al. integrated this chip with a microcontroller ATMega128 and an XBee wireless transceiver [11]-[13].

Researchers from Los Alamos National Lab have worked on a series of wireless SHM sensor systems embedded with Analog Device's impedance analyzer chips AD5933 for years and developed the third generation of the sensor system called Wireless Impedance Device (WID-3) in 2009 [14]-[16].

Our team also developed a series of impedance-based SHM systems using Texas Instrument DSP and low-power microcontroller unit (MCU) evaluation boards [4]-[6]. We employed three methods to reduce power consumption of our impedance-based SHM systems. These three methods are reviewed in the following sections.

- **On-board Data Processing**

The major source of power consumption for a wireless sensor node is the radio. For example, a microcontroller unit MSP430 from Texas Instruments used for our SHM sensor node in [4] dissipates 3 mW under a low-power operation mode, while a low-end radio CC2500 from Texas Instruments embedded in the sensor node dissipates 65 mW during transmission. So, it is essential to reduce the radio transmission time for a low-power wireless SHM sensor node. We adopted an on-board data processing approach for our SHM sensor node in [4], which processes the data on the board and sends only the final outcome (healthy or damaged) of the SHM operation to the control center.

- **Elimination of a DAC for generation of an excitation signal**

A sinusoidal signal sweeping a certain frequency range is usually used to excite a PZT patch for the impedance-based method. Sampled values of a sinusoidal signal are pre-stored in a memory, and a DAC reproduces the corresponding analog signal. This method is straightforward, but it requires a DAC and a large memory space for a large frequency sweeping range. Our method is to use a rectangular pulse train rather than a sinusoidal signal. A rectangular pulse train illustrated in Figure 2-1 (a) has a duty cycle of 0.5, and its fundamental frequency (which is given as $1/t_p$, where t_p is the pulse period) sweeps a certain desired frequency range. The Fourier transform of a pulse train with a pulse period t_p and the duty cycle of 0.5 has odd harmonics kf_o, k=1, 3, 5 …, where $f_o = 1/t_p$. Figure 2-1 (b) illustrates frequency components of a pulse train with the fundamental frequency ranging from 40 kHz to 50 kHz. The magnitude of the third harmonic is about

33 percent of the fundamental frequency, and the fifth one about 20 percent.

A rectangular pulse train is digital, and hence a processor can directly generate such a signal. Hence, a DAC is eliminated for our system to save power. One potential issue is existence of harmonics on the signal. Since both the baseline and measured impedance profiles are under the subject of the same frequency terms, the sensitivity for the detection metric may not be affected by harmonics. Our experimental results in [5] reveal that use of a rectangular pulse train does not incur any noticeable deterioration of the performance for the impedance method.

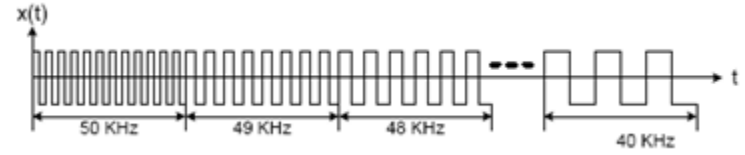

(a) Time domain

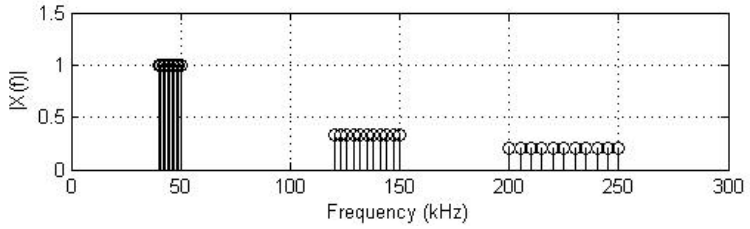

(b) Frequency domain

Figure 2-1. Rectangular pulse train

- **Elimination of an ADC for response signal sensing**

Existing methods, such as one employed by Analog Device's impedance analyzer chips, sample the response signal using an ADC and performs an FFT to extract the impedance component of the frequency. A typical ADC used for an SHM system consumes large power, possibly next to a radio and a processor, and FFT is also computationally intensive to increase power dissipation. Our method is to eliminate an ADC and the FFT operation by sensing the phase, not the magnitude, of the response signal.

The electrical admittance is expressed as $Y(jf) = G(f) + jB(f)$, where $G(f)$ and $B(f)$ are conductance and susceptance terms, respectively. It is known that the conductance term of a PZT patch is more sensitive to damage [17]. Let $G_{base}(f)$ denote the baseline

conductance obtained from a healthy structure and $G_{SUT}(f)$ be the conductance of a structure under test (SUT). The difference of the two conductance terms $G_{base}(f)$ - $G_{SUT}(f)$ is used for existing impedance-based SHM systems to detect damage. Assuming all parameters are constant, our earlier work showed that

$$G_{base}(f) - G_{SUT}(f) \approx C \sin[\phi_{base}(f) - \phi_{SUT}(f)] \quad (1)$$

where C is a constant, and $\phi_{base}(f)$ and $\phi_{SUT}(f)$ are the phase of the baseline admittance and the SUT admittance, respectively [18]. Expression (1) suggests that the difference of the phases, instead of the conductance $G(f)$'s, can be sensed for the impedance method.

The phase of an admittance $\phi(f)$ for a frequency f can be expressed as in (2), where $T_d(f)$ is the time difference between the voltage and the current:

$$\phi(f) = 2\pi f \times T_d(f) \quad (2)$$

When both the voltage and current are represented as binary signals, the time difference $T_d(f)$ of the two signals is obtained using an exclusive-OR (XOR) operation as illustrated in Figure 2-2. For details, refer to [4].

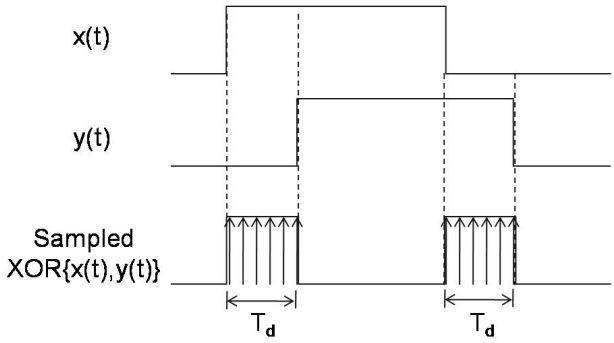

Figure 2-2. Phase difference measured by sampling the output of the XOR operation

- **Damage Metric**

The damage metric (DM) for our system is defined as a normalized absolute sum-of-differences between the phase profiles of the baseline and of the SUT given by

$$\mathrm{DM} = \frac{\sum_{f_i=f_l}^{f_h} |\phi_{base}(f_i) - \phi_{SUT}(f_i)|}{M(f_l, f_h)} \tag{3}$$

where $M(f_l, f_h)$ is the number of frequency points from the lowest frequency f_l to the highest frequency f_h. The DM of a SUT is compared against a threshold value, whose value may be set based on field experience. If the DM is lower than the threshold value, the SUT is considered healthy. Otherwise, it is damaged. It is important to note that fixed-point calculations without involving multiplications or division are sufficient for Expression (3) provided $M(f_l, f_h)$ is set to power of 2. So, a simple fixed-point processor, rather than a floating-point processor, can be used for our SHM system to save power. Adoption of a more sophisticated DM is possible for our system to improve the SHM performance, but it is not the objective of our system.

2.2.2 Lamb wave SHM System

A Lamb wave SHM system uses a piezoelectric transducer, specifically a PZT patch, to launch an elastic wave into a structure, and the response signal is sensed by the same PZT patch or another attached somewhere else on the structure [7],[8]. A self-contained Lamb wave system typically comprises three functional blocks: a signal actuation block, a signal sensing block, and a signal processing block. The signal actuation block is comprised of a DAC, which generates an analog signal from a waveform stored in memory. This analog signal is then amplified and applied to a PZT patch attached to the structure. The response signal picked up by a PZT patch is usually amplified, sampled, and digitized by an ADC. Finally, the signal processing block processes the received response, and the received signal is compared against a baseline to determine whether or not damage exists in the system. A signal processing block typically employs a general purpose processor, a DSP chip, or an MCU.

To design a Lamb wave system, it is important to determine an optimal driving frequency for the structure under test. The excitation waveform also plays an important role in determining the effectiveness of a Lamb wave system. One of the most commonly employed excitation waveforms is a tone burst sine wave with a Hanning window, which is a raised-cosine with a roll-off factor of 1. Because a Hanning

windowed sinusoid has low bandwidth, the generated Lamb waves are limited to their fundamental modes [10]. Figure 2-3 shows an excitation waveform in both the time domain and the frequency domain.

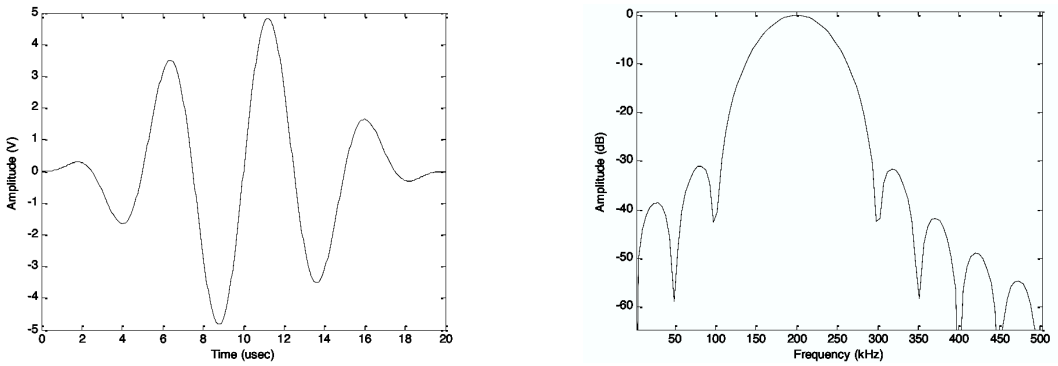

(a) Excitation Waveform in time domain (b) Normalized Frequency Spectrum

Figure 2-3. 200 kHz excitation waveforms

A discrete wavelet transformation (DWT) is typically used to reduce noise [19],[20]. DWT is a special case of the wavelet transform that provides a compact representation of a signal in time and frequency, and it can be computed efficiently. The DWT is defined in the following expression:

$$W_{\Psi}(j,k) = \sum_{j}\sum_{k} s(n)2^{-j/2}\Psi_{j,k}(2^{-j}n-k) \tag{4}$$

where $\Psi_{j,k}$ is called as mother wavelet with finite energy. The flexibility of choosing a proper mother wavelet is one of the strongest advantages of using DWT. If we choose the mother wavelet as the excitation signal itself and the dilation coefficient $j = 0$, the DWT results in the correlation between the excitation signal and the sensed signal, which is simple to compute.

The DM used for our system is a normalized absolute sum of difference between the DWT of the baseline or reference signature and the DWT of the sensed signature from the structure under test. The DM indicates the amount of deviation of the sensed signature from the baseline. The DM increases with the damage level and is ideally zero for a structure without damage. The DM is expressed as follow:

$$DM = \frac{\sum_{i}\left|WT_{current}(i) - WT_{baseline}(i)\right|}{\sum_{i}\left|WT_{baseline}(i)\right|} \tag{5}$$

where $WT_{current}$ and $WT_{baseline}$ denote DWT of the sensed and baseline waveforms, respectively. $|x|$ denotes the absolute value of x.

2.2.3 Acoustic Emission Sensor

When a material structure is distorted or damaged by an external or internal force, it releases energy in the form of ultrasonic vibrations, and this phenomenon is termed acoustic emission (AE) [21]. Due to the fact that a stress causes acoustic emission, AE is also referred to as Stress Wave Emission. Since most AE sources are damage-related, detection and monitoring of these emissions are commonly used to predict material and structural failure [22],[23]. Acoustic emissions emanating from within the structural materials can provide information about growing cracks and deformation of structures and adverse chemical reactions, such as corrosion. By analyzing AE information, small-scale damage is detectable long before failure, so that AE can be employed for non-destructive evaluation (NDE) in aeronautics, mechanical engineering, and civil infrastructure systems to find defects during structural proof tests and plant operation.

An acoustic emission sensor generates an electrical signal proportional to the AE level. An AE sensor enables detection of low level sonic and ultrasonic signals generated by impacts of meteorites or space debris for our system. Key performance parameters of an AE sensor are sensitivity, compatibility, and low power consumption for our system. We have selected an acoustic sensor PK15I from the Physical Acoustics Corporation (PAC) for our system [24]. Specifications of the AE sensor are summarized below in Table 1. The sensitivity of an AE sensor is represented as "dB ref 1V/μbar" (1 bar = 0.987 atm $\approx 10^5$ N/m^2). The unit represents the generated voltage over the reference that is 1V per 1 μbar, and a larger value represents higher sensitivity. The sensitivity of our sensor is -36 dB ref V/μbar, which means it generates $10^{-1.8}$ V under the application of pressure 1μbar. Typical AE sensors for industry applications have around -60 dB ref 1V/μbar [24],[25], and the sensitivity of highly sensitive AE sensors is around -30 dB ref 1V/μbar. Our sensor PK15I provides reasonably high sensitivity (-36 dB ref 1V/μbar) and is well suited to the repetitive laboratory tests and experiments.

Table 2-1. Specification of Acoustic Sensor PK15I

Dynamic Parameters	
Peak Sensitivity	-36 dB ref V/μbar
Operating Frequency	50 ~ 200 KHz
Environmental	
Temperature Range	-35 ~ 80 °C
Shock Limit	500 g
Physical Parameters	
Dimension	20.6 cm (diameter) x 27
Weight	51 g
Case Material	Stainless steel
Connector	SMA
Electrical Parameters	
Input Voltage Range	4 ~ 7 V
Operating/Max Current	5/35 mA
Internal Preamp Gain	26 dB

2.3 Proposed AED System

We describe the operation and a prototype of our AED system in this section, which integrates an AE sensor with two SHM systems, the impedance-based and the Lamb wave.

2.3.1 System Operation

The objective of our AED system is to deliver an integrated structural health monitoring system, which uses acoustic emission to detect adverse impacts, the impedance method to monitor structural integrity, Lamb wave method to assess surfaces. An acoustic sensor monitors acoustic emission continuously, while the impedance-based and the Lamb wave systems are in sleep mode. When the acoustic sensor detects an impact, it wakes up the impedance-based SHM, which determines if the impact incurred damage. When damage is detected, it activates the Lamb wave SHM system to determine the severity and location of the damage. The flow chart of the AED system is shown in

Figure 2-4.

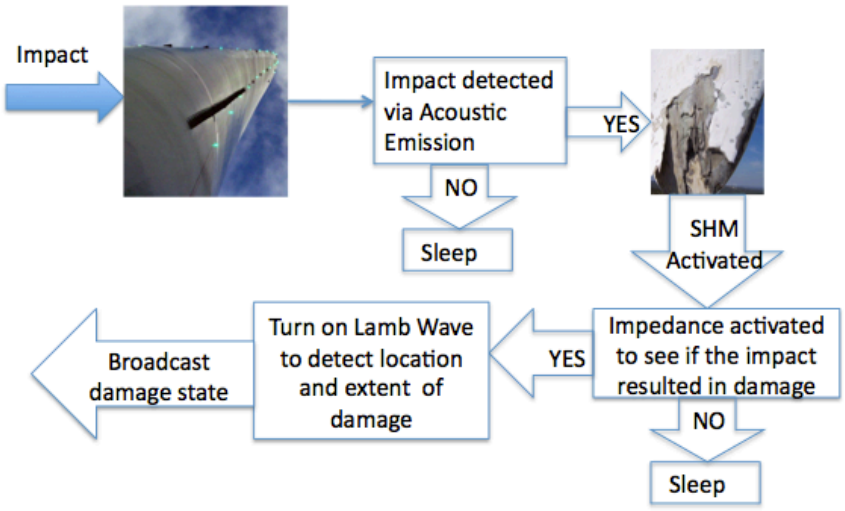

Figure 2-4. Flow chart of the AED system

2.3.2 Prototype

A prototype of our AED system is based on a TMS320F2812 DSP evaluation board from Texas Instruments [26]. TMS320F2812 is a 32-bit fixed point DSP supporting up to 150 million instructions per second (MIPS). Figure 2-5 (a) shows the block diagram of the AED system. The impedance-based and the Lamb wave systems share the DSP board for signal processing and control. The RS232 interface provides communication between the SHM system and a Graphical User Interface (GUI) program running on a host PC. Figure 2-5 (b) shows our prototype. The five blocks in Figure 2-5 (a) are labeled as “A” through “E” in Figure 2-5 (b). Figure 2-6 shows acoustic sensor PK151 attached to an aluminum plate, which monitors acoustic emission on the plate.

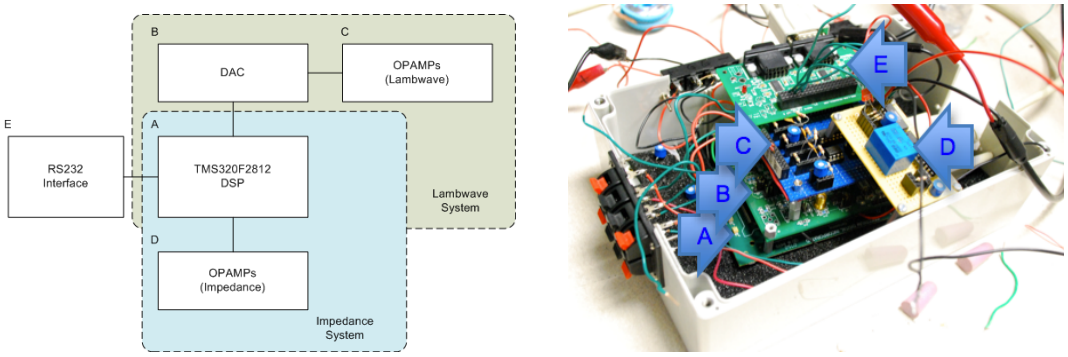

(a) Block Diagram (b) Prototype

Figure 2-5. Block Diagram and a Prototype of the AED system

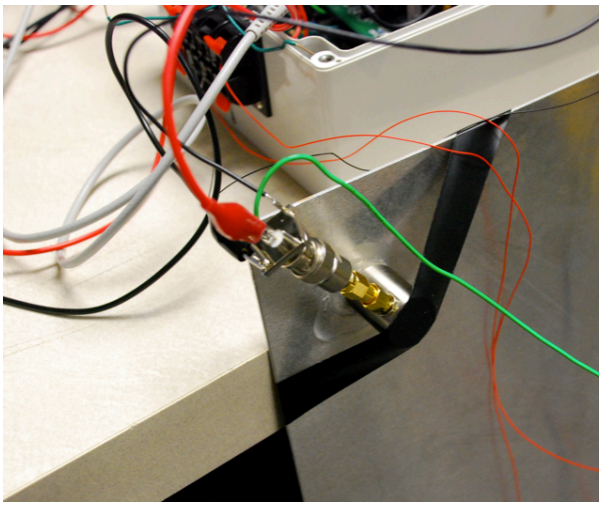

Figure 2-6. Acoustic sensor attached on an aluminum plate

2.4 Experimental Results

We present the test environment and experimental results of our AED system in this section. We use an aluminum plate as a test structure and conducted experiments with the prototype described in the above.

2.4.1 Test Environment

Figure 2-7 (a) shows two PZT patches on an aluminum plate. The PZT labeled as "1" is for the Impedance-based SHM system and called named PZT #1 hereafter, and The PZT labeled as "2" is for the Lamb wave system called PZT #2. We obtained the baseline profiles for both the impedance-based SHM system and the Lamb wave system for the

health structure. Then, we made a 4″x2″ hole at six inches away from PZT #2 as shown in Figure 2-7 (b), and the hole emulates damage.

To emulate an adverse event on the specimen, a light stroke with a small hammer (with 1/4 lb head weight) is applied to the aluminum plate. The AE sensor generates a signal with the peak voltage of 0.5 V, which wakes up an Impedance-based SHM system.

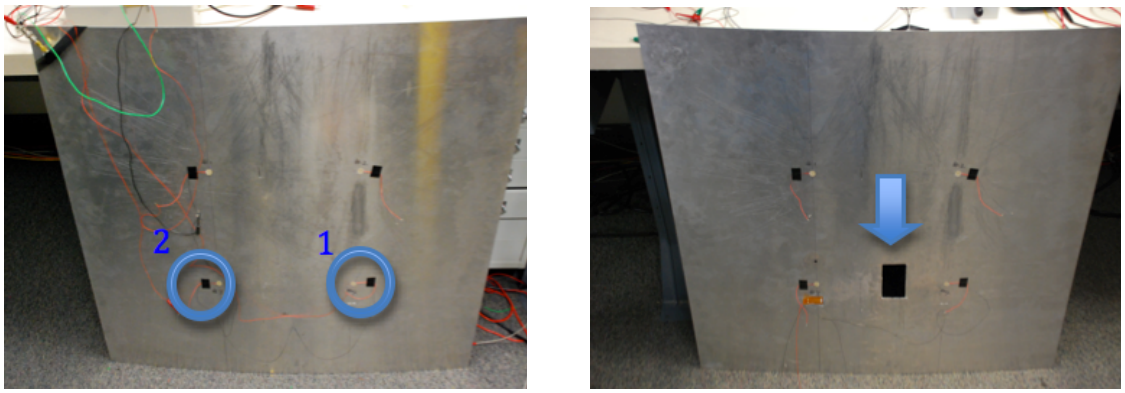

(a) Health structure (b) Structure with damage

Figure 2-7. Aluminum plate as a test structure

2.4.2 Impedance-Based SHM

We empirically obtained the excitation frequency range of 8 KHz to 150 KHz of the test structure using an impedance analyzer, in which the magnitude of the impedance has many peaks. As noted in Section 2.1, our impedance-based SHM measures the phase of the admittance. Figure 2-8 (a) and (b) show the phase profiles of the healthy and damaged structures, respectively. As can be seen from the two pictures, the two phase profiles are significantly different to demonstrate the effectiveness of the proposed method. The DM for our system is normalized absolute sum-of-differences. The DM is obtained to be 29 for this particular damage and exceeds the threshold value of 10 (which was obtained through experiments) to initiate the Lamb wave system.

(a) Healthy structure (b) Damaged structure

Figure 2-8. Phase profiles of the healthy and damaged structures

2.4.3 Lamb wave SHM

The excitation signal for our system was obtained through experiment. It is a tone burst 200 KHz sine wave with a Hanning window under a raised-cosine of a roll-off factor of 1, and the waveform and its frequency spectrum are shown in Figure 2-3. The top waveform in Figure 2-9 is a wavelet-transformed baseline signal for the healthy structure measured by PZT #2. The bottom waveform in the Figure 2-9 is a wavelet-transformed signal for the damaged structure measured by the same PZT patch. The major difference between the two waveforms is the signal encircled in the bottom figure, which is an echo signal reflected at the perimeter of the damage hole. The arrival time of the echo signal is 56.32 μs, and the surface velocity measured for the aluminum is 0.2125 in/μs. So, the distance to the damage is obtained as 5.984 inches (= ½ × 56.32 μs × 0.2125 in/μs), which is close to the actual distance.

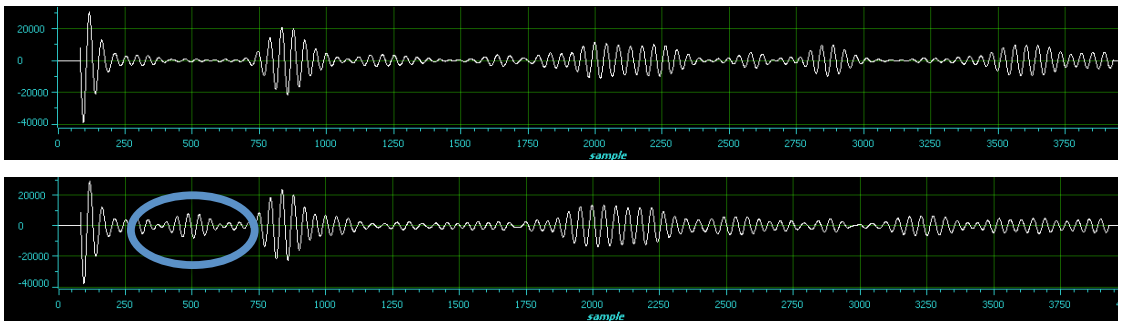

Figure 2-9. Wavelet transformed Lamb wave signals (a) baseline, (b) currentline

2.5 Conclusion

We presented our Adverse Event Detection (AED) SHM system, which integrates an acoustic sensor, impedance-based and Lamb wave SHM systems. An acoustic sensor detects impacts, which activates the impedance-based SHM. When damage is detected by the impedance-based SHM system, it activates the Lamb wave SHM system to determine the severity and location of the damage present. An acoustic sensor continuously monitors acoustic events, while the impedance-based and the Lamb-wave SHM systems are in sleep mode. The two SHM systems are activated only when there is an acoustic event. Therefore, use of an acoustic sensor reduces overall power dissipation of our AED system.

We developed a prototype using a Texas Instruments TMS320F2812 DSP evaluation board to demonstrate the feasibility of our method. Experiment results successfully verified the proof of concept for the proposed system. The proposed method can be effective for space applications, in which meteorites and space debris may cause structural damage and low power consumption is critical.

Chapter 3: Adverse Event Detection (AED) System of Wind Turbine Blade with Wireless Sensor Network

In this chapter, the AED system has been applied to a Wind Turbine Blade (WTB). The main difference between the previous AED system in Chapter 2 and the one that will be explored in Chapter 3 is that several sensor nodes are deployed throughout the WTB specimen, and each sensor is configured in a sensor network topology.

In this study, assuming that many sensor nodes need to be deployed due to the 100 meters long WTB, the wireless sensor network system has been devised enabling a host PC to gather and analyze all the results collected from sensor nodes. In addition, thanks to the introduction of the Acoustic Emission (AE) sensor, this wireless sensor network offers an even further power-optimized solution to Structural Health Monitoring (SHM) operations.

Throughout the following sections, the concepts of the AED system and the wireless sensor network are dealt with, and the prototype verifies these concepts are feasible to be physically implemented.

3.1 Introduction

To monitor and control the fatigue lifespan of a WTB, the integrated SHM system combining the AE sensor and the impedance-based SHM has been devised. The AE sensor attached to the integrated system serves as the initial starter of the SHM operation. The integrated SHM system in this study has two main features: the first invokes the impedance-based SHM only when the AE sensor detects any impact imposed on the specimen, and the second sends the SHM result to the host PC through a wireless communication channel. From these functionalities, we could obviate unnecessary power losses by skipping unwanted repetitions of a power hungry impedance-based SHM, and we can deploy as many sensors as possible onto the specimen to conduct more precise evaluations of the SHM without worrying about a power consumption. Our SHM system

has been realized using a MSP430 microcontroller from TI [27] as a base station, and proved to successfully detect damage on the specimen. Chapter 3 is organized as follows: Section 2 describes preliminaries to establish the AED system. In section 3, the proposed AED system with the wireless sensor network is described at both a system level and component level. Section 4 presents the experimental results of the AED system on the WTB. Finally, the AED system is summarized and concluded in section 5.

3.2 Preliminaries

In this section, we review the WTB and the wireless sensor network used for our system.

3.2.1 Wind Turbine Blade

The WTB is the rotor part of a Wind Turbine (WT) that is converts wind energy into electricity. Since the effectiveness of WT is proportional to the WTB's length and the reciprocal of the WTB's weight [28], the current WTB is designed to be around 100 meters long in diameter and to consists of light-weighted materials such as fiberglass and other composite materials in order to increase the efficiency of the WT.

While the wider but light-weighted WTB enables an effective WT, the amount of fatigue that the WTB receives from the wind source has increased incurring a shorter life cycle of the WTB. As the blade failure can cause other parts of the WT to be broken and even damage nearby WTs [29], the continuous monitoring of the WTB is necessary in order to prevent any adverse event, and the SHM offers the exact features that satisfy the needs while monitoring the WTB and helping prevent any further damage from developing.

3.2.2 Wireless Sensor Network for SHM

Continuous monitoring techniques for structural systems, such as civil or mechanical structures, have been researched in an effort to maintain structures in the same condition as when they were first established. Furthermore, these techniques help

prevent any disastrous event that can cause any casualties. To implement a continuous monitoring system, one of the general methodologies that have been used for real structures is a sensor network, where sensors are deployed throughout a structure and a communication link is established among sensors to collect and send each sensor's output to the host PC. For instance, a few hundred sensors have been deployed throughout the Tsing-Ma suspension bridge in Hong Kong, and all sensors were connected to the host PC via coaxial wires. Although this system offers the exact function that monitors the state of the bridge and detects any adverse event on the bridge before a catastrophe occurs, the cost for this wire-connected system is expensive and labor-intensive with respect to the initial setup and maintenance [1].

To address these limitations, a wireless sensor network have been suggested, where each sensor's role has been extended from a mere transducer, which can sense and quantify an analog event, to a wireless transceiver that can interact wirelessly among sensors and the host PC. Due to the fact that coaxial wires can be totally removed from the monitoring system, the wireless sensor network can offer a significantly lower cost for the initial setup and management. Although the initial motivation for the wireless sensor network stemmed from the lower cost, it is each sensor's autonomous computing power that makes the wireless sensor network one of the most promising methodologies in the SHM systems [1]. Using the microcontroller's computing power, each sensor is able to actively collect information regarding damage on the structure, and analyze the information to assess whether a real damage occurs.

The sensor that is equipped with a transducer, a transceiver, and a microcontroller is often referred to as the sensor node. Other components that are common in the sensor node's configuration are the Digital-to-Analog Converter (DAC) for an actuating interface and the Analog-to-Digital Converter (ADC) for converting analog signals into a digital form. As for the sensor network topologies for wireless sensor networks, the star, the peer-to-peer, and the two-tier topologies are generally used [1],[30].

3.3 Proposed AED System

In this section, the operating algorithm for our AED system is presented, and the prototype system and sub-components of the prototype are described.

3.3.1 System Operation

Our integrated SHM system is based on the MSP430 microcontroller from the Texas Instruments [27]. The MSP430 is a 16-bit Reduced Instruction Set Computing (RISC) CPU supporting up to 16 million instructions per second (MIPS) operations. The maximum core operating clock frequency is 16 MHz and can be reduced down to 32 KHz to be used for the low power operation mode. The supply voltage for this microcontroller is ranging from 1.8 V to 3.6 V. If 16 MHz is set up for the main clock frequency, over 3.3 V should be provided.

As shown in Figure 3-1, the entire SHM system consists of five main structures. The AE sensor (#1) detects any impact imposed on the specimen. The AE interface circuit located between the AE sensor and the MSP430 provides the output of the AE sensor with an adequate biasing voltage (1.0 V in this study) and protects the MSP430 from an unexpected spike that would damage the MSP430. The impedance method circuit for the SHM (#4) executes the impedance-based SHM with the help of MSP430's computing power. Once the analysis of the impedance-based SHM is finalized, the result should be sent from the MSP430 to the host PC (or the center node #6). The host PC can invoke another MSP430 to perform an impedance-based SHM at a different PZT for further evaluations of the SHM on the specimen.

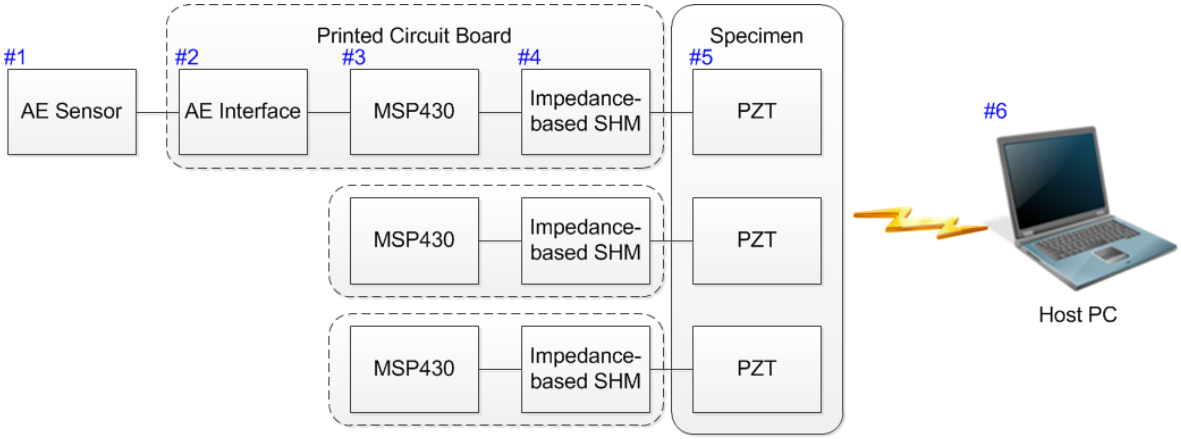

Figure 3-1. The SHM system diagram

Owing to the fact that the MSP430 is capable of a wireless communication with a 2.4 GHz RF transceiver, our SHM system was developed as a wireless sensor network system as shown in Figure 3-2. In conventional impedance-based SHMs, each sensor node should wake up in a certain amount of time to perform its SHM operation whether there is real damage or not. Compared with the conventional system, each sensor node of our system can safely remain in the 'SLEEP' mode due to the introduction of the AE sensor that wakes up the sensor node only when it detects any suspicious impact. Once the sensor node in contact with the AE sensor finishes its impedance-based SHM operation, it sends the evaluation result to the center node, which sequentially wakes up another sensor node to command them to start its impedance-based SHM operation. Owing to this functionality, each sensor node does not have to run a timer in the MSP430 to calculate the time when it should wake up, and our SHM system is able to reduce power consumption that would dissipate using timer operations.

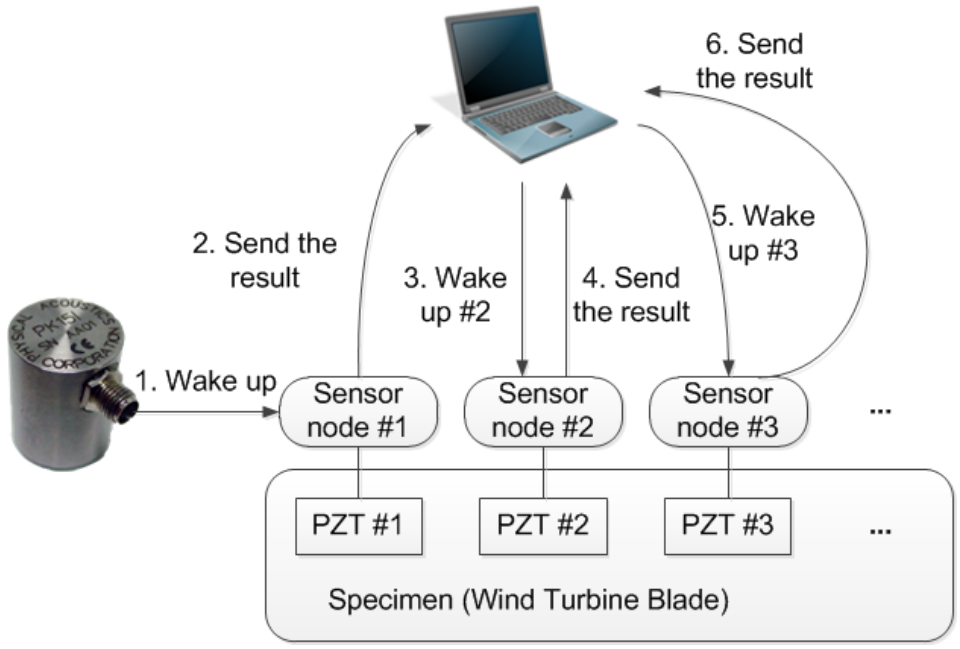

Figure 3-2. Wireless Sensor network SHM system

In our system, although only three MSP430s are deployed throughout the specimen, the number of sensor nodes can be expanded depending on the sensor deployment resolution varying with the specimen's physical dimension.

3.3.2 Prototype

As discussed in the preliminary section, the key feature enabling our SHM system to reduce its total power is to remove power hungry AD/DA converters from the impedance-based SHM, and to introduce the AE sensor to the sensor network system. By the nature of dealing with analog signals, AD/DA converters need a certain level of sampling resolution that consumes a few hundred mW [31], so that removing converters allows us to reduce a significant amount of power consumption in our SHM system. Furthermore, eliminating AD/DA converters makes the firmware of the MSP430 simple and concise to be coded. The introduction of the AE sensor helps reduce the power consumption by enabling each sensor node to be in the 'SLEEP' mode for the most of SHM life cycle consuming a small amount of power (~ 2.1 μW) [27].

- **Impedance Circuit**

The excitation and sensing part of our SHM system are shown in Figure 2-1. The MSP430 generates a train of rectangular pulses, which is applied to a PZT patch. The OPAMP output voltage $V_o(t)$, which represents the current through the PZT patch, is converted into a binary signal by the comparator. The binary signal and the input voltage $V_i(t)$ are compared using an exclusive-OR (XOR) gate to measure the phase difference of the two signals, i.e., the voltage and the current of the PZT patch.

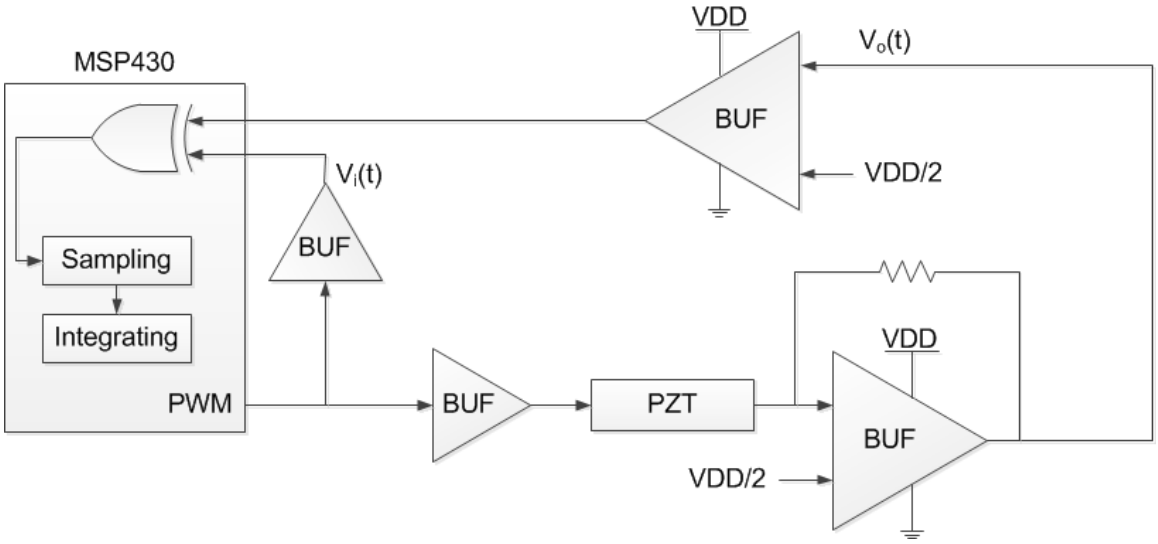

Figure 3-3. System Architecture for Impedance Method

- **AE sensor and interface**

Once the SHM system receives a signal reasonably large enough to be estimated as an impact from the AE sensor, it wakes up from the 'SLEEP' mode and starts its impedance-based SHM procedure to detect damage. To sort out a relatively large signal, 200 mV_{peak} was selected as a criterion, and one comparator was used to implement it. Figure 3-4 shows the comparator setting to screen out a signal that has over 200 mV_{peak}. When the AE sensor recognizes any acoustic wave on the surface of the specimen, it amplifies the acoustic wave with a 26 dB gain, and then the AE sensor outputs this amplified signal with the 1 V biasing voltage. Therefore, if the AE sensor carries any signal larger than 200 mV_{peak}, the B(+) is going to have an input voltage larger than 1.2 V, and the comparator will eventually produce a '1' on its output port. This comparator

output is connected with one unused General Port Input/Output (GPIO) of the MSP430 to be used for waking up the MSP430 from the 'SLEEP' mode.

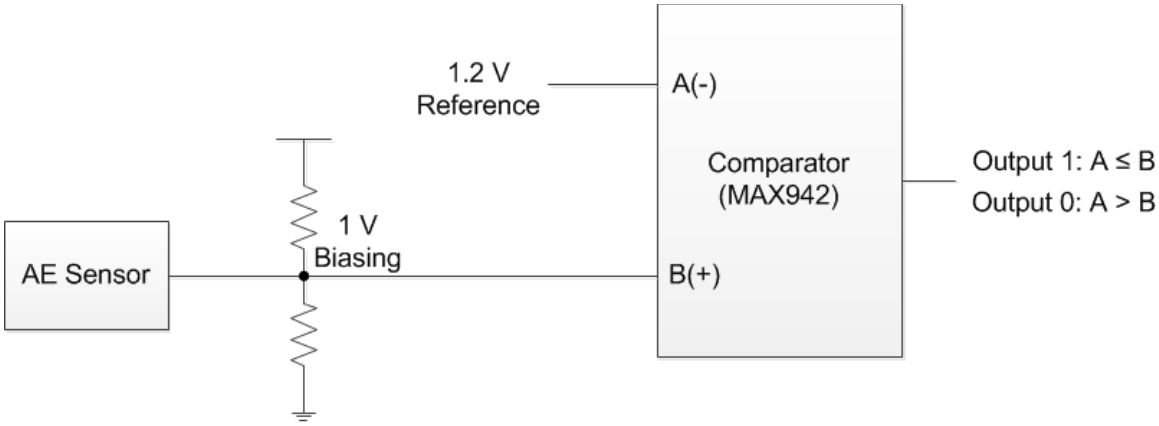

Figure 3-4. Comparator Setting with AE Sensor

We devised the AE interface circuit that is placed between the AE sensor and the MSP430. The main functions of this interface circuit are a) to provide the AE sensor with a supply voltage (5V), b) to bias the AE sensor's output signal with 1 V, c) to implement the low-pass filter for removing high frequency terms, d) to protect the MSP430 from a sudden voltage spike, and finally e) to detect a signal over 200 mV_{peak}. Each circuit corresponding to each function is shown in Figure 3-5.

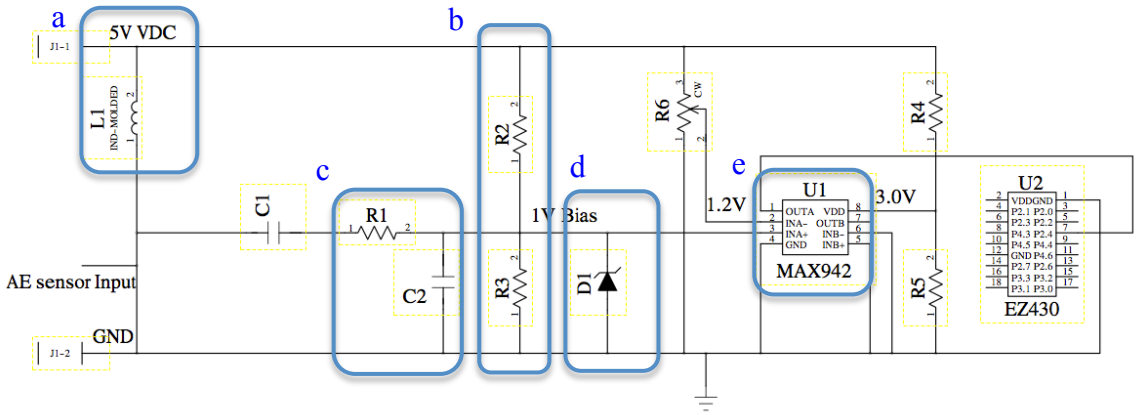

Figure 3-5. Circuit Diagram for the AE interface

The whole circuit of our SHM sensor node including the AE sensor interface, the

MSP430, and OPAMPs for the impedance-based SHM circuit is drawn in Figure 3-6.

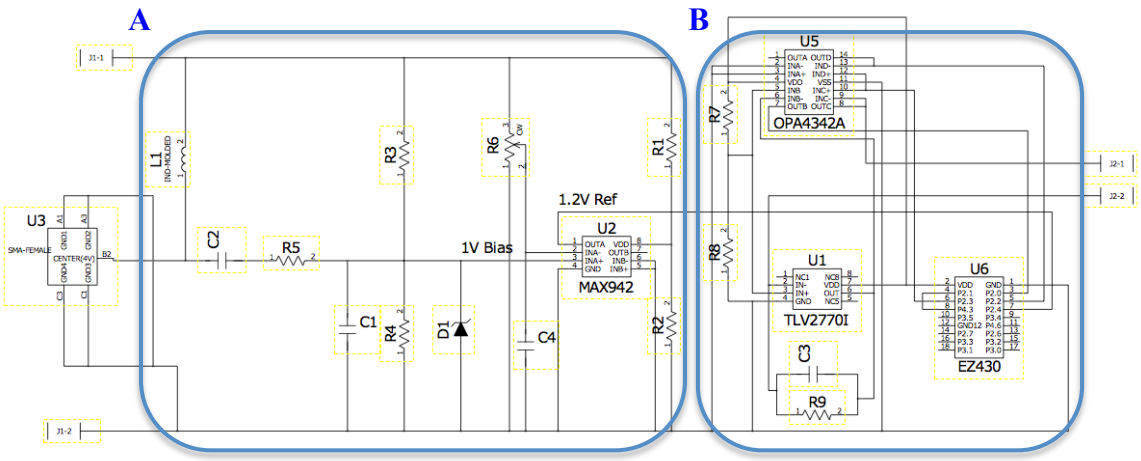

Figure 3-6. Circuit diagram for the sensor node (A: AE interface circuit , B: Impedance-based SHM circuit with MSP430)

The circuit diagram above was converted into the Printed Circuit Board layout as depicted in Figure 3-7, and the manufactured PCB is shown in Figure 3-8.

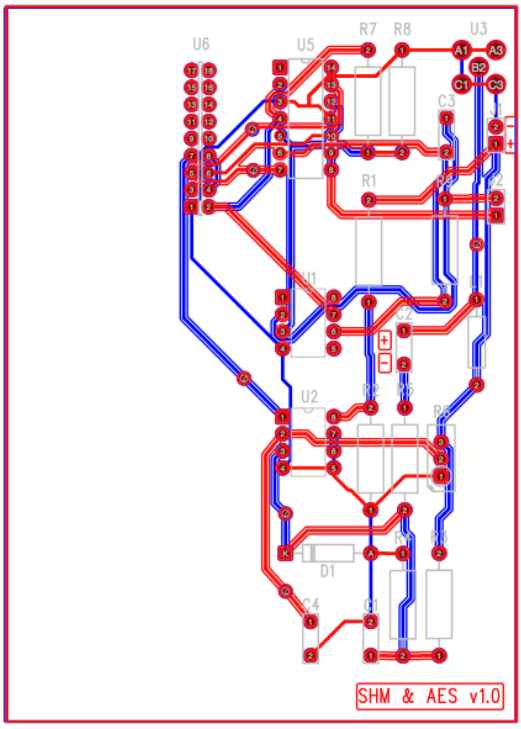

Figure 3-7. PCB layout for the sensor node

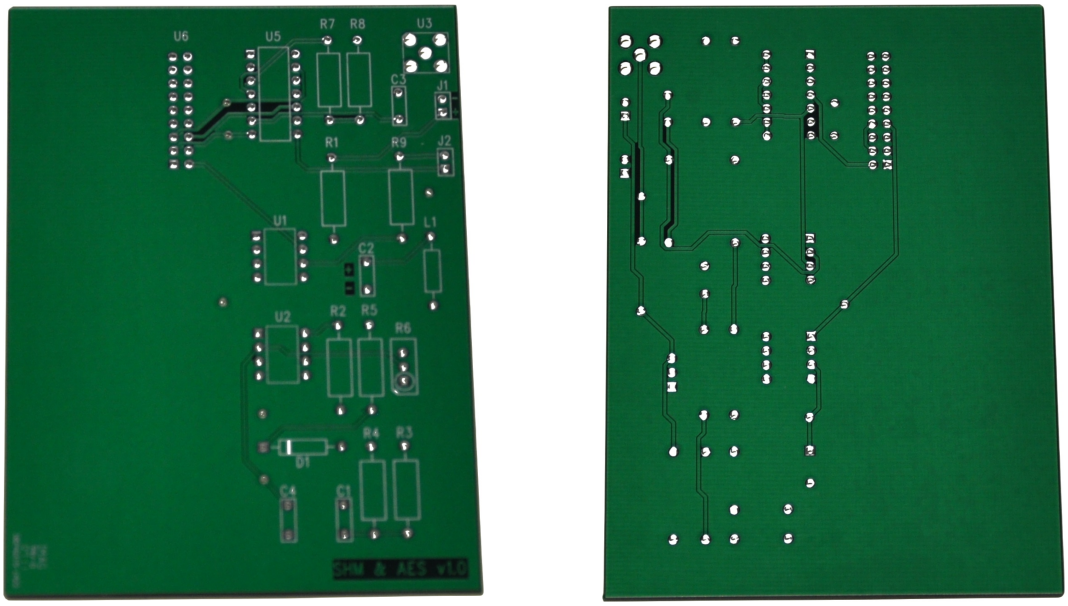

(a) Front-side (b) Back-side

Figure 3-8. Manufactured PCB for the sensor node

The assembled PCB with the MSP430 microcontroller is depicted in Figure 3-9.

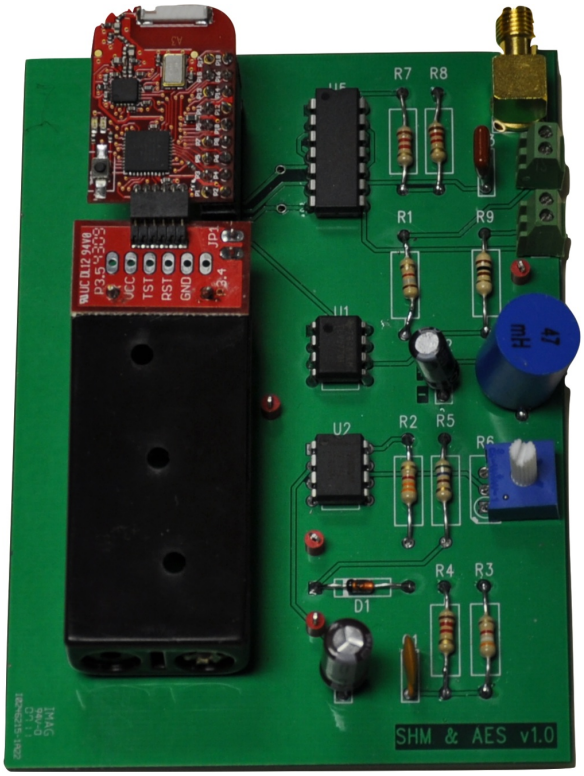

Figure 3-9. Assembled PCB to be used for a sensor node

3.4 Experimental Results

The prototype of the AED system was installed on the WTB. This prototype starts its operation with an impact on the WTB, and each sensor sends its own SHM analysis results to the host PC. The experimental setup and quantitative results are presented in this section.

3.4.1 Test Environment

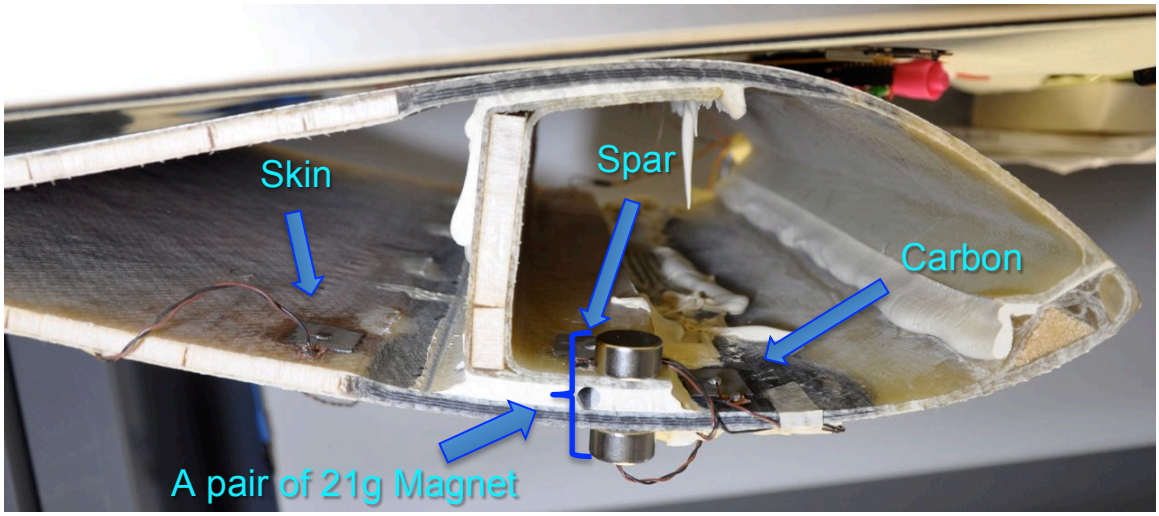

Figure 3-10. Demo setting on Wind Turbine Blade with three PZTs

To execute the SHM operation on our specimen, we attached 3 PZTs onto the specimen. The PZT patches used for our SHM testing are roughly 2 x 2 cm^2 and are made from the PSI-5H4E material from the Piezo Systems, Inc. They were deployed in three locations on the specimen that are shown in Figure 3-10. The left patch location is above the balsa skin section near the balsa/carbon intersection and will be referred to as the skin patch. The patch in the middle is on the fiberglass spar flange and will be referred to as the spar patch. Finally, the patch on the right is on the carbon fiber spar cap and will be referred to as the Carbon patch [28]. To emulate damage on the specimen, a pair of 21g magnets was used.

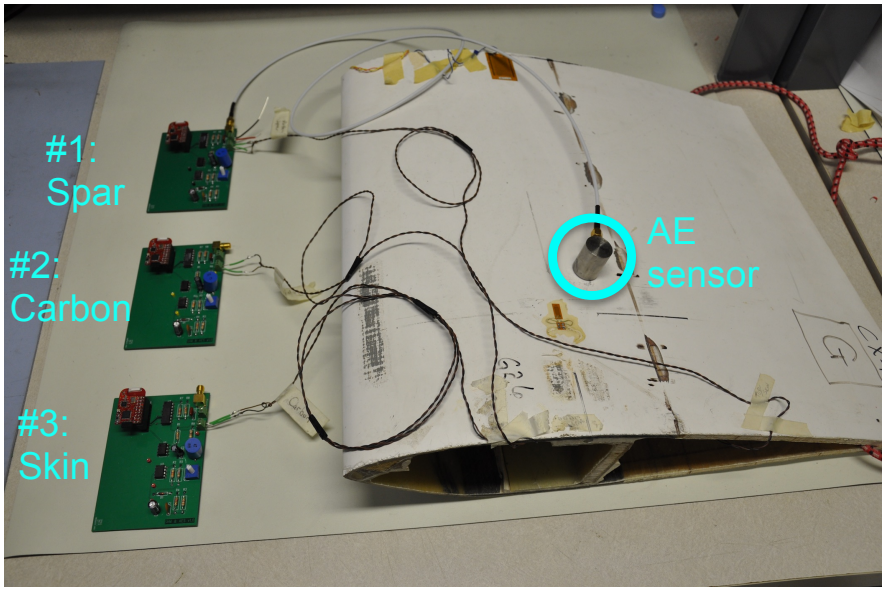

(a) PZTs and AE sensor setup

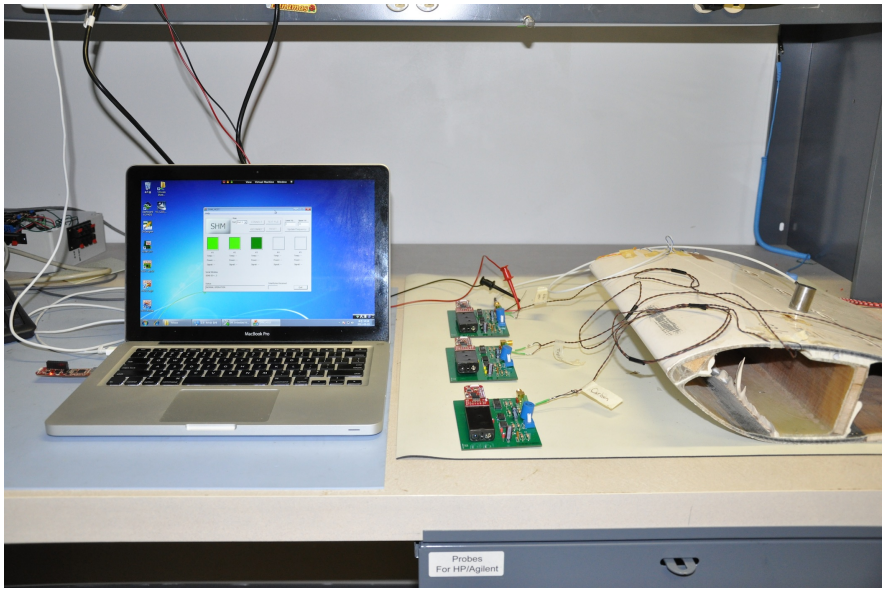

(b) The entire demo setup

Figure 3-11. Demo Setup

As the system diagram is depicted in Figure 3-11 (a), three sensor nodes were attached to each PZT while the AE sensor was mounted onto the surface of the WTB and connected to only the sensor node attached to the spar position. Each sensor node calculates the baseline signature once it receives power from battery. To emulate an impact on the specimen, a light stroke with a small hammer (with a 1/4 lb head weight)

was applied on the surface of the specimen. For our SHM experiment, we used a sweeping frequency range from 5 KHz to 15 KHz, within which the phase changed most sensitively to damage.

To remotely monitor each sensor node's SHM result, a GUI program for the host PC was developed as well. As shown in Figure 3-12, each empty rectangle shows each sensor node's status: #1 for the sensor node attached to the spar position, #2 for the carbon position, and #3 for the skin position. When this rectangle blinks in a green color, it means that there is no damage detected, while a red color means there is the damage detected.

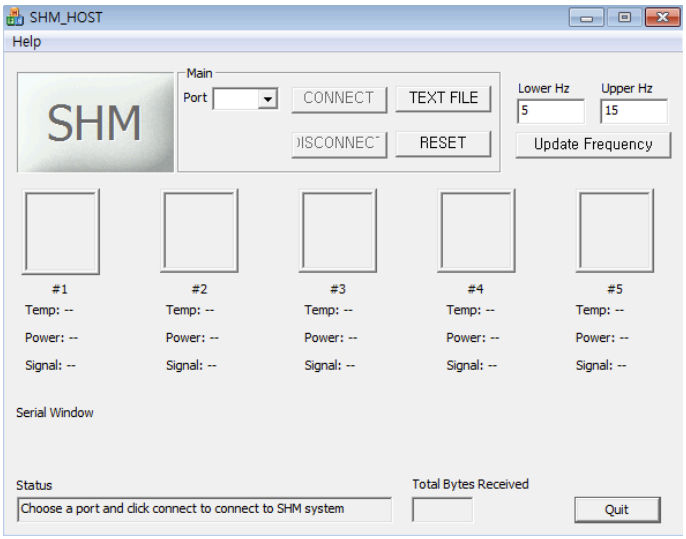

Figure 3-12. GUI Interface Program

3.4.2 Impedance-Based SHM with Wireless Sensor Network

- **Download Baseline**

To download baseline signatures measured from each PZT, we simply connected a battery pack to each sensor node. Once powered by battery, each sensor node started downloading the baseline signature into its internal memory.

Once finished, the GUI showed three green lights indicating that all sensor nodes worked fine and had not detected any damage yet.

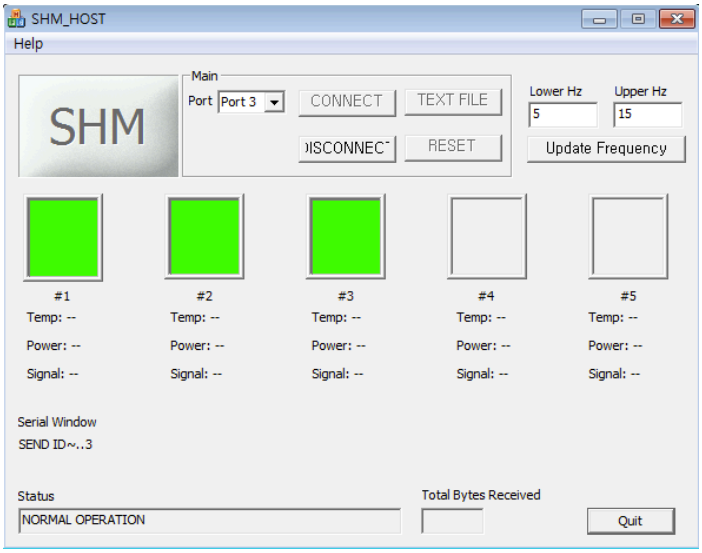

Figure 3-13. GUI screen captured for the initial setup

• When damage applied

By attaching a pair of magnets on the spar position, we applied damage to the specimen. After applying damage, we stroke the surface of the specimen using a small hammer with 1/4 lb head weight to give an impact to the AE sensor. Once the AE sensor caught an acoustic wave generated by the stroke, the AE sensor woke up the first sensor node to execute the impedance-based SHM if the sensed signal had over 200 mV_{peak}. The actual acoustic wave and the comparator output that resulted in waking up the first sensor node was measured and represented in Figure 3-14. As shown in this figure, the comparator produced high signals (blue) only when the acoustic wave (yellow) rose above the 1.2 V reference voltage (green) as described in Section 3.3.

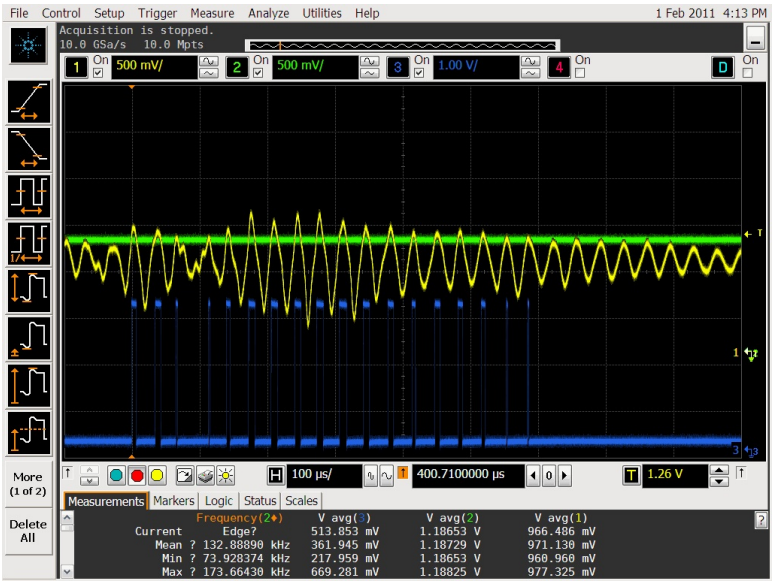

Figure 3-14. The Acoustic wave and the comparator output (Acoustic wave: Yellow, Comparator output: Blue, 1.2 V reference voltage: Green)

Once the host PC received the result from the first sensor node, it woke up the second sensor node to start the SHM function. The same sequence was applied for the third sensor node. As shown in Figure 3-15, since the damage applied at the spar area, the lamp for the first sensor node connected to the spar patch showed a red light indicating that the damage was detected.

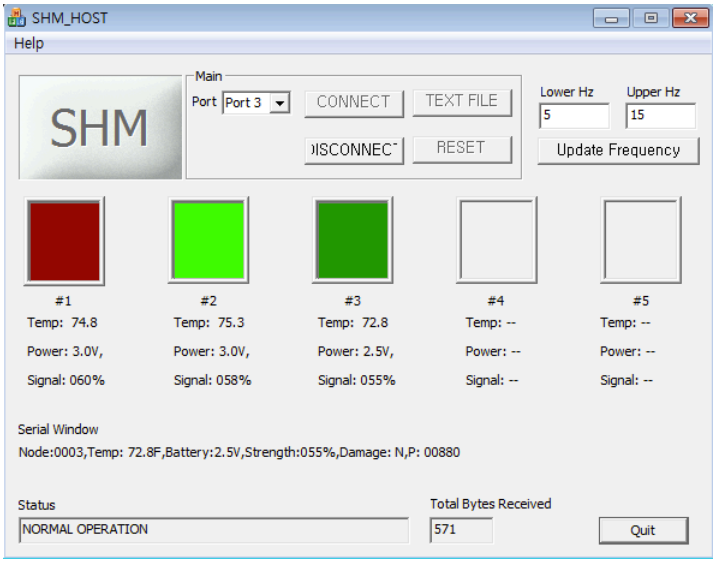

Figure 3-15. GUI screen captured after applying damage at the Spar position

In Table 2, DM results calculated from each sensor node were tabulated. Inside of the sensor nodes, '15' was set as the DM threshold value to determine if damage occurred. The table shows that only the spar sensor node's DM had a value larger than the threshold representing that the spar sensor node detected damage. Each sensor node evaluated the DM five times, and used the average value of those as the final DM.

Table 3-1. Damage Metric measured from each sensor node (Threshold value = 15)

DM #	Spar	Carbon	Skin
1	18	10	9
2	19	10	9
3	19	10	8
4	19	10	9
5	19	10	9
avg	18.8 (>15)	10 (<15)	8.8 (<15)

• When damage removed

To remove damage from the specimen, a pair of magnets was detached from the spar area. To run each sensor nodes' SHM operation, we applied the small stroke again. Since the damage was cleared, all lamps of GUI show green lights indicating that there was no damage on the specimen.

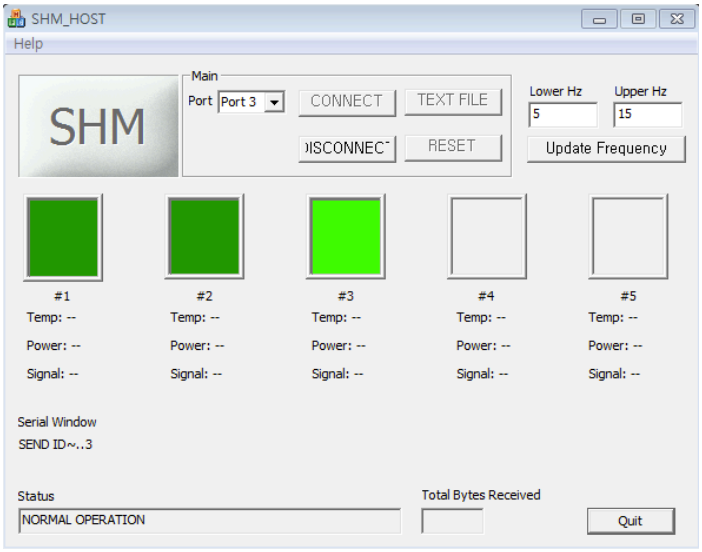

Figure 3-16. GUI screen after removing damage from Spar position

3.5 Conclusion

The AED system was applied to the WTB to monitor its structural health status so that precautious actions can be taken before further damage develops onto the WTB. Sensor nodes with the capability of the impedance-based SHM were deployed throughout the WTB, and with the help of the AE sensor and the wireless sensor network, the power efficient SHM system was realized and confirmed through our prototype.

Chapter 4: Conclusion

As one of various Non-Destructive Examination (NDE) methods, the SHM has been intensively researched to find effective ways to monitor a structure of interest. By virtue of the SHM, a structural condition can be managed and controlled to be as rigid and concrete as its first established condition. According to earlier studies and implementations, the SHM system was implemented by deploying sensors throughout the structure of interest and connecting those sensors with coaxial wires. While this implementation was able to provide exact functionalities that were expected for the SHM, the significant installation cost and the labor-intensive nature hindered this configuration from being widely considered as an effective SHM. To overcome these limitations, the sensor node that is equipped with an RF transceiver and a microcontroller has been suggested. Owing to its wireless transmission capability and computing power, the coaxial wires are no longer needed, and the need for human labor resources is not significant any more.

Since the impedance-based SHM and the Lamb wave SHM are the most commonly accepted methods for assessing a structural healthiness, many efforts have been made to embed these methods into the sensor node such that each sensor node can execute its pre-installed SHM methods and assess a structural damage by itself. This autonomous sensor node enables a more accurate analysis of a structural healthiness.

While the autonomous sensor nodes on the SHM system suggest a promising future of the SHM, the limitation of a power source for sensor nodes imposes another challenge to render a sensor node power efficient. In this thesis, the AED system was proposed to address this issue.

In Chapter 1, the AED system was devised to integrate the AE sensor, the impedance-based SHM, and Lamb wave SHM. The AE sensor detects impacts, which activates the impedance-based SHM. When the damage is detected by the impedance-based SHM system, it activates the Lamb wave SHM system to determine the severity and location of the damage present. The AE sensor continuously monitors acoustic events, while the impedance-based SHM and the Lamb-wave SHM systems are in the ‘SLEEP’

mode. The two SHM systems are activated only when there is an acoustic event. Therefore, the use of the AE sensor reduces the overall power dissipation of our AED system.

In Chapter 2, the AED system was applied to the WTB to monitor its structural health status so that precautious actions can be taken before further damage develops onto the WTB. Sensor nodes with the capability of the impedance-based SHM were deployed throughout the WTB, and with the help of the AE sensor and the wireless sensor network, the power efficient SHM system was realized and confirmed through our prototype.

Prototypes developed from Chapter 1 and Chapter 2 confirm that the AED system is feasible and ready to apply to the real site of interest that needs an SHM system for structural maintenance and safety.

References

[1] Jerome P. Lynch, Kenneth J. Loh (2006), "A Summary Review of Wireless Sensors and Sensor Networks for Structural Health Monitoring," The Shock and Vibration Digest, Vol 38, No 2, March 2006

[2] J.K. Kim, D. Zhou, D.S. Ha, and D.J. Inman, (2009), "A Practical System Approach for Fully Autonomous Multi-Dimensional Structural Health Monitoring," SPIE International Symposium on Smart Structures and Materials & Nondestructive Evaluation and Health Monitoring, Vol. 7292-56, (10 pages), March.

[3] A. Raghavan, and C. E. S. Cesnik, (2007), "Review of Guided-wave Structural Health Monitoring," The Shock and Vibration Digest, 39(2), 91-114.

[4] D. Zhou, D.S. Ha, and D.J. Inman, (2010), "Ultra Low-Power Active Wireless Sensor for Structural Health Monitoring," International Journal of Smart Structures and Systems, Vol. 6, No. 5-6, pp. 675-687, July/August.

[5] Kim, J., Grisso, B. L., Ha, D. S., and Inman, D. J., (2007), "An All-digital Low-power Structural Health Monitoring System". IEEE Conference on Technologies for Homeland Security, 123-8.

[6] Kim, J., Grisso, B. L., Ha, D. S., and Inman, D. J., (2007), "A System-On-Board approach for Impedance-based Structural Health Monitoring" Proceeding of SPIE, Vol. 6529, 65290O, San Diego, March.

[7] Wait, J.R., Park, G., Sohn, H. and Farrar, C.R., (2004), "Plate Damage Identification Using Wave Propagation and Impedance Methods," *Proc. of SPIE*, vol. 5394, pp. 53-65.

[8] Swartz, R.A., Flynn, E., Backman, D., Hundhausen, R.J. and Park, G., (2006), "Active Piezoelectric Sensing for Damage Identification in Honeycomb Aluminum Panels," *Proceedings of 24th Intl. Modal Analysis Conference.*

[9] S. Deyerle, D.S. Ha, and D.J. Inman, (2010), "A Low-Power System Design for Lamb Wave Methods," SPIE International Symposium on Smart Structures and Materials & Nondestructive Evaluation and Health Monitoring, Vol. 7650, 765019 (8 pages), March.

[10] J. G. Proakis, and D. G. Nanolakis, (2007) Digital Signal Processing, Prentice Hall.

[11] Park, S., Shin, H., and Yun, C., (2009), “Wireless impedance sensor nodes for functions of structural damage identification and sensor self-diagnosis”, Smart Mater. Struct., 18- 055001.

[12] Park, S., Yun, C., Inman, D. J., and Park, G., (2008), “Wireless Structural Health Monitoring for Critical Members of Civil Infrastructures Using Piezoelectric Active Sensors”, Proceeding of SPIE, Vol. 6935, 69350I, San Diego, March.

[13] Park, S., Lee, J., Yun, C., and Inman, D. J., (2008), “Electro-Mechanical Impedance-Based Wireless Structural Health Monitoring Using PCA-Data Compression and k-means Clustering Algorithms”, Journal of Intelligent Material Systems and Structures, Vol. 19, No. 4, 509-520.

[14] Overly, T.G., Park, G., Farinholt, K.M., Farrar, C.R., (2008), “Development of an extremely compact impedance-based wireless sensing device,” Smart Mat. and Struct., (17) 6: 065011.

[15] Mascarenas, D. L., Todd, M. D, Park, G. and Farrar, C. R., (2007), “Development of an impedance-based wireless sensor node for structural health monitoring” Smart Mater. Struct. (16) 6: 2137–2145.

[16] Taylor, S.G., Farinholt, K.M., Park, G. and Farrar C. R., (2009), “Impedance-Based Wireless Sensor Node for SHM, Sensor Diagnostics, and Low-Frequency Vibration Data Acquisition” Proc. of 7th International Workshop for Structural Health Monitoring, Palo Alto, CA, September.

[17] Park, G., Sohn, H., Farrar, C. R., and Inman, D. J., (2003), "Overview of piezoelectric impedance-based health monitoring and path forward", The Shock and Vibration Digest, 35, 451-463.

[18] Kim, Jina., (2007), “Low-Power System Design for Impedance-Based Structural Health Monitoring”, PhD Dissertation, Virginia Tech.

[19] S. Legendre, D. Massicotte, J. Goyette et al, (2000), ““Wavelet-Transform-Based Method of Analysis for Lamb-Wave Ultrasonic NDE Signals,” IEEE Trans. on Inst. and Meas., 49(3), 524-530.

[20] H. P. Sohn, W. G., J.R., N. P. Limback et al, (2004), “Wavelet-based active sensing for delamination detection in composite structures,” Journal of Smart Materials and Structures, 13, 153-160.

[21] Yuxin Qin, Yijun Liang, Yinghao Zhang, Guang Zhang, (2010), "Experimental Study on an Optical Fiber Acoustic Emission Sensor Array" Academic Symposium on Optoelectronics and Microelectronics Technology and 10th Chinese-Russian Symposium on Laser Physics and Laser Technology.

[22] Ákos Lédeczi, Thomas Hay, Péter Völgyesi, D. Robert Hay, András Nádas, and Subash Jayaraman, (2009), "Wireless Acoustic Emission Sensor Network for Structural Monitoring" IEEE SENSORS JOURNAL, VOL. 9, NO. 11, NOVEMBER.

[23] R. K. Miller, (2006), "Acoustic emission testing," in *Nondestructive Testing Handbook*, 3rd ed. Columbus, OH: Amer. Society for Non-Destruc- tive Testing, vol. 6.

[24] www.pacndt.com

[25] www.aesensor.co.uk , www.vallen.de/products/sensors.htm

[26] TMS320F2812 Digital Signal Processor Data Manual, Texas Instruments Inc., May 2006.

[27] MSP430x2xx Family User Guide, Texas Instruments Inc., SLAU144E 2008

[28] Corey Wilson Pitchford, "Impedance-Based Structural Health Monitoring of Wind Turbine Blades," Master thesis at Virginia Tech, August 2007

[29] Simmermacher, T., James, G. H., and Hurtado, J. E. 1997. "Structural Health Monitoring of Wind Turbines." Proceedings of the International Workshop on Structural Health Monitoring, Stanford, CA, September 18-20, 1997, 788-797.

[30] Soojin Cho, Chung-Bang Yun, Jerome P. Lynch, Andrew T. Zimmerman, Billie F. Spencer Jr., Tomonori Nagayama, "Smart Wireless Sensor Technology for Structural Health Monitoring of Civil Structures," Steel Structures 8 267-275, 2008

[31] Jina Kim, Benjamin Grisso, Dong Ha, Daniel Inman, "Digital Wideband Excitation Technique for Impedance-Based Structural Health Monitoring System," ISCAS 2007